

See discussions, stats, and author profiles for this publication at: <https://www.researchgate.net/publication/265476855>

# Electronic Structure of Self-Assembled Monolayers Modified with Ferrocene on Gold Surface: Evidences of Electron Tunneling

ARTICLE in THE JOURNAL OF PHYSICAL CHEMISTRY C · SEPTEMBER 2014

Impact Factor: 4.77 · DOI: 10.1021/jp506425c

CITATIONS

2

READS

52

6 AUTHORS, INCLUDING:



**Filipe Camargo Dalmatti Alves Lima**

University of São Paulo

6 PUBLICATIONS 6 CITATIONS

SEE PROFILE



**Arrigo Calzolari**

Italian National Research Council

108 PUBLICATIONS 1,901 CITATIONS

SEE PROFILE



**Marilia J Caldas**

University of São Paulo

116 PUBLICATIONS 1,718 CITATIONS

SEE PROFILE



**Helena Petrilli**

University of São Paulo

71 PUBLICATIONS 670 CITATIONS

SEE PROFILE

# Electronic Structure of Self-Assembled Monolayers Modified with Ferrocene on a Gold Surface: Evidence of Electron Tunneling

Filipe C. D. A. Lima,<sup>†</sup> Arrigo Calzolari,<sup>‡</sup> Marília J. Caldas,<sup>†</sup> Rodrigo M. Iost,<sup>§</sup> Frank N. Crespilho,<sup>§</sup> and Helena M. Petrilli<sup>\*,†</sup>

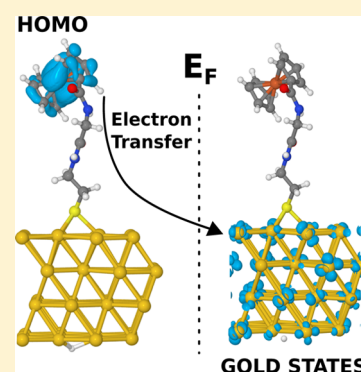
<sup>†</sup>Departamento de Física dos Materiais e Mecânica, Instituto de Física, Universidade de São Paulo, 05508-090 São Paulo, SP, Brazil

<sup>‡</sup>CNR-NANO Istituto Nanoscienze S3 National Center, I-41125 Modena, Italy

<sup>§</sup>Instituto de Química de São Carlos, Universidade de São Paulo, 13560-970 São Carlos, SP, Brazil

## S Supporting Information

**ABSTRACT:** The electron transfer mechanism for the prototypical system ferrocenoyl-glycylcystamine (Fc-Gly-CSA) on Au(111) is investigated within the framework of density functional theory. Different Fc-Gly-CSA/Au systems, including the explicit methanol solvent and sodium perchlorate counterion, are studied. As seen from the partial density of states, electronic contributions close to the Fermi energy are found to derive only from the ferrocene units and gold atoms, while the contributions from electronic states located on the molecular spacers (Gly-CSA) are detected at lower energies, with or without the effects of the environment. These results strongly indicate a direct ferrocene-to-gold tunneling as the electron transfer mechanism across the interface.



## INTRODUCTION

As a major multidisciplinary field, the study of electron transfer (ET) reactions is considered a fundamental step toward the realization of efficient molecular electronics devices. In the context of heterogeneous charge transfer, there is high interest in using ferrocene (Fc) due to its electrochemical capability to reversibly oxidize and reduce at low voltages (<0.5 V). Self-assembled monolayers modified with ferrocene molecules (Fc-SAMs) have been considered as good models<sup>1</sup> since they show well-defined structures in terms of thickness and composition.<sup>1–7</sup> A good SAM/metal interface should realize an efficient donor–acceptor system, where an electro-active headgroup (e.g., Fc) is connected to the metallic electrode (e.g., Au) through a molecular spacer. Oligopeptides modified with thiol groups are suitable candidates to act as molecular bridges. Indeed, it has been proved that they may provide a stable anchor to Au surfaces and a good control in the experimental data capture.<sup>1–3,8–23</sup>

Among the plethora of experimental results in the literature on Fc-SAMs, particularly relevant are the studies by Kraatz and co-workers,<sup>3,15,24</sup> who reported a comprehensive set of experimental investigations, which include the functionalization of the ferrocene modified with glycine (Gly) and cystamine (CSA) (ferrocenoyl-glycylcystamine)<sup>25</sup> and other spacer molecules.<sup>20,24</sup> The direct measurement of ET rates through Fc-decorated peptides using nonpolar amino acids (Gly, Val, and Ala), CSA, and helical oligopeptides<sup>21</sup> has been performed,<sup>12</sup> along with the characterization of their electronic properties by means of X-ray absorption spectra (XAS).<sup>14</sup>

Finally, the modifications of the reorganization energy in the presence of different salts have been recently investigated.<sup>3,15</sup>

On the theoretical side, ET can be explored in the context of the Marcus theory,<sup>1,26,27</sup> which provides a major breakthrough to the evaluation of the electron transfer rates. However, despite the huge amount of studies, the charge transfer mechanism in Fc-SAMs is still controversial. Empirical models proposed electronic tunneling,<sup>21,22,28</sup> electronic hopping,<sup>4,10,16,29</sup> and/or a combination of the two,<sup>18,30</sup> as a function of the distance between the active headgroup (Fc) and the electrode. Even though theoretical studies based on molecular dynamics reported on the determination of redox potentials,<sup>31</sup> the structural properties of SAMs,<sup>32,33</sup> the influence of salt counterions,<sup>34</sup> Marcus' ET parameters,<sup>35</sup> and ion-pair formation,<sup>34</sup> the ultimate ET mechanism has not been unambiguously identified yet. Quantum mechanical calculations<sup>14,35–37</sup> investigated the ET mechanism on self-standing Fc-terminated molecules but neglected the fundamental interaction with the metal substrate.

Here we present an ab initio study, in the framework of the Kohn–Sham (KS) density functional theory (DFT),<sup>38</sup> of the electronic structure of the Fc-Gly-CSA on the Au(111) surface, aiming at providing further insights on the evaluation of the ET mechanism between the Fc-SAMs and the gold substrate. The density of states (DOS), KS probability densities, and energy

Received: June 27, 2014

Revised: September 6, 2014

Published: September 9, 2014



levels of Fc-Gly-CSA derived systems are systematically analyzed in different configurations, as a SAM on the Au substrate, with and without the presence of methanol solvent and sodium perchlorate ( $\text{NaClO}_4$ ) salt. Even though DFT does not include any direct kinetic process, the resulting electronic structure provides a clear scenario for the identification of a direct electron transfer from Fc to gold, which does not involve any intermediate step along the peptide spacer. This may help the understanding of the electrochemical properties of such complex systems that can be tuned for the realization of proper electrochemical devices.

## THEORETICAL METHODS

We start characterizing the Gly-CSA and Fc-Gly-CSA molecular samples in the gas phase that we assume as a reference in the analysis of the interfaces. In the crystalline form,<sup>25</sup> the Fc-Gly-CSA monomers dimerize, forming cystamine units, linked by a S–S bond. During the formation of the interface the S–S bond breaks,<sup>3,12</sup> leaving two radicals that attach to the gold substrate through the thiol ending groups. In our simulations, the gas-phase molecules are considered in the fully saturated neutral form, resulting from the full bonding of the sulfur atom to a hydrogen (Figure 1a). The Gly-CSA unit is simulated in the same way, substituting the Fc head with a methyl termination.

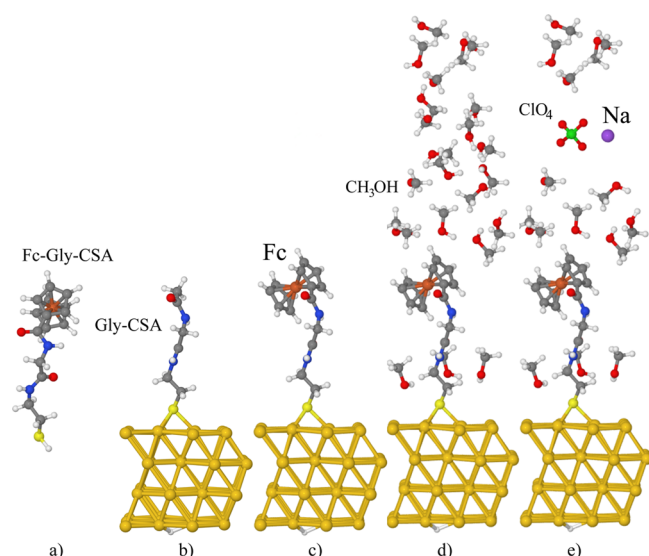


**Figure 1.** Schematic view of (a) Fc-Gly-CSA in the gas phase and (b–e) molecular systems adsorbed on the gold surface: (b) Gly-CSA/Au(111); (c) Fc-Gly-CSA/Au(111); (d) Fc-Gly-CSA/Au(111) in methanol solvent; (e) Fc-Gly-CSA/Au(111), sodium perchlorate, and methanol solvent. Atom colors: yellow (Au), light yellow (S), green (Cl), gray (C), blue (N), orange (Fe), red (O), white (H), violet (Na). Notice that the Au(111) surface is continuous and infinite in 2D (supercell approach).

The H atom that saturates these molecules has no role in the formation of the interface with gold, thus, in the preparation of the interface configurations, we considered the adsorption of the molecules in the radical form. In order to ensure an overall even number of electrons in the supercell, a H atom is included on the other side of the Au surface, as shown in Figure 1. We have tested that the slab is sufficiently wide, so this does not perturb the structural and electronic properties of the target molecule/metal interface.

In order to gain a systematic control on the different interactions that rule the experimental setup,<sup>3</sup> we studied a set of molecule/Au(111) interfaces, increasing the complexity of the system step by step. First, we considered the Gly-CSA/Au(111) interface (Figure 1b), to characterize the formation of the S–Au interface in the absence of the Fc headgroup. Ferrocene is next included in the simulations as shown in Figure 1c. Then, we considered the effect of the environment including methanol solvent (Figure 1d). Finally, as sodium perchlorate is always diluted in the experimental samples—in order to balance the formation of  $\text{Fc}^+$  upon charge transfer—a  $\text{Na–ClO}_4$  pair is also included in our simulations (Figure 1e). As experimental results<sup>3,12</sup> do not exhibit any preferential surface, we have chosen the Au(111), which is the standard for this kind of investigation.<sup>39–41</sup>

Calculations were performed within the DFT framework, as implemented in the QUANTUM ESPRESSO suite of codes.<sup>42</sup> We employed the generalized gradient approximation (GGA) in the PBE formulation<sup>43</sup> for the exchange correlation functional. Ionic potentials were described by ab initio ultrasoft pseudopotentials in the Vanderbilt's form.<sup>44</sup> Au(5d) electrons are explicitly treated in the valence shell. Single-particle wave functions and electron density are expanded in a plane-wave basis set with an energy cutoff of 28 and 280 Ry, respectively. A regular  $(4 \times 4)$  grid of k-points was used to sample the 2D Brillouin zone of the interfaces. Molecular systems were treated at the  $\Gamma$ -only level.

All systems are simulated using periodically repeated supercells with dimension  $(10.2 \times 8.8 \times 40.6) \text{ \AA}^3$ . The slab contains four layers of Au(111), each layer forming a  $(3 \times 2\sqrt{3})$  two-dimensional (2D) supercell and one molecule (with and without Fc) as shown in Figure 1. In the absence of the solvent, all structures have been optimized until atomic forces were smaller than 0.02 eV/Å. The molecule ionization potential (surface work function) is calculated in the KS approximation as the difference between the ferrocene HOMO (gold Fermi level) and the vacuum level, respectively. The latter is evaluated from the double averaged electrostatic potential, resulting from the self-consistent DFT calculation in the spatial region far away from the systems.<sup>45,46</sup> Only single-point calculations were done in the presence of the solvent and salt, as shown in Figure 1d and Figure 1e. Starting from the optimized Fc-Gly-CSA/Au interface of Figure 1c, the solvent has been explicitly simulated by including 23 methanol molecules in the cell, using the chemical builder VegaZZ<sup>47</sup> code, which creates a cage around the initial system where the solvent is further parametrized in terms of intermolecular interactions, such as distances, angles, vdW interactions, and H-bonds, obtained empirically. The salt ion is placed 14 Å from the Fc iron in order to prevent spurious direct interactions between Fc and salt, with 15 methanol molecules filling the super cell.

## RESULTS AND DISCUSSION

The electronic density of states in the energy region near the gap of the isolated Gly-CSA and Fc-Gly-CSA are summarized in Figure 2. The two spectra are aligned to the lowest occupied molecular orbital (LOMO) of the common Gly-CSA unit. The occupied frontier orbitals of the Gly-CSA fragment have a  $\pi$  character, and while the HOMO ( $H_m$ ) has a remarkable contribution from the oxygen lone pairs and is mostly distributed on the peptide chain, the lowest unoccupied molecular orbital LUMO ( $L_m$ ) spreads mostly to the thiol termination. The molecule has a Kohn–Sham (KS) HOMO–

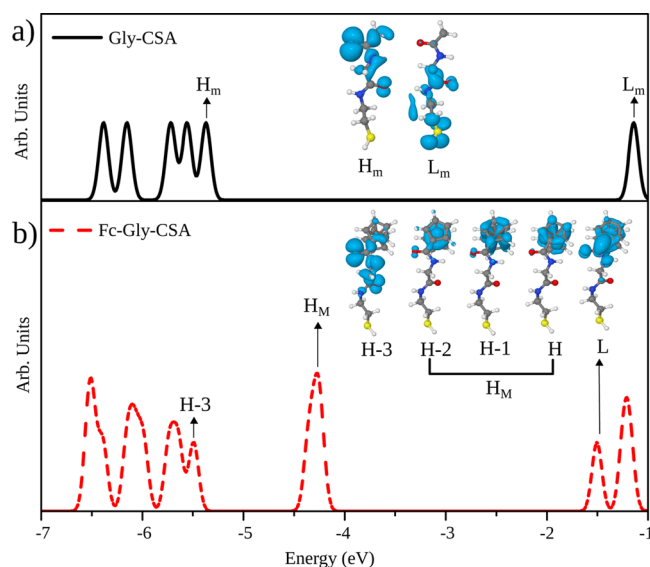


**Figure 2.** DOS of (a) Gly-CSA and (b) Fc-Gly-CSA molecules in the gas phase. Insets are isosurface plots of selected KS orbitals.

LUMO gap of 4.2 eV. The effect of ferrocene (Figure 2b) is 2-fold: (i) it imparts a shift of the occupied Gly-CSA frontier orbitals toward higher binding energies and (ii) introduces a manifold of occupied states ( $H_M$ ) in the pristine gap of the Gly-CSA unit. This leads to an effective reduction of the gap to 2.7 eV. The HOMO manifold is constituted of three KS states localized on Fc only (formally HOMO, HOMO-1, and HOMO-2 states), with no component along the peptide. Orbital H-3, which is formally the HOMO-3 state of the system, derives from the HOMO orbital ( $H_m$ ) of Gly-CSA (Figure 2a) only partially hybridized with Fc. The net spatial separation of the orbitals, localized either on the Gly-CSA or in the Fc subsystems, will play a crucial role in the electron transfer processes discussed below.

In order to decouple the effects due to the S-Au chemical bond at the interface and the presence of the ferrocene on the electronic structure, we considered the adsorption of the Gly-CSA fragment on the Au(111) surface, as shown in Figure 1b. The starting configuration was obtained setting the Gly-CSA molecule almost vertically, with respect to the Au(111), with the thiol group in a “top” position and 2.8 Å from a surface Au atom. After geometry optimization, the Gly-CSA moved to a “hollow” position, forming 3-fold S-Au bonds (2.34, 2.43, and 2.46 Å, respectively). This corresponds to a binding energy of -1.37 eV/molecule, which is a clear fingerprint of a chemisorption interaction. This behavior is similar to the cysteine case on the Au(111) substrate reported in the literature.<sup>41</sup> We see also a small positive charge associated with the sulfur atom in contact with the surface, in keeping with the chemical bonding picture (Table S1, Supporting Information).

The DOS of the Gly-CSA/Au(111) interface is shown in Figure 3. The energy range closer to the Fermi energy is dominated by the sp band of the gold substrate, modified by the formation of the S-Au bonds. Representative KS orbitals of these S-Au coupling states are displayed in the inset of Figure 3. We can see the level splitting  $H_m$ /S-Au states, induced by the bonding to the surface, noting the similarity between these two orbitals, both derived from the HOMO ( $H_m$ ) state of the isolated molecule. Also, we find a splitting with deeper valence

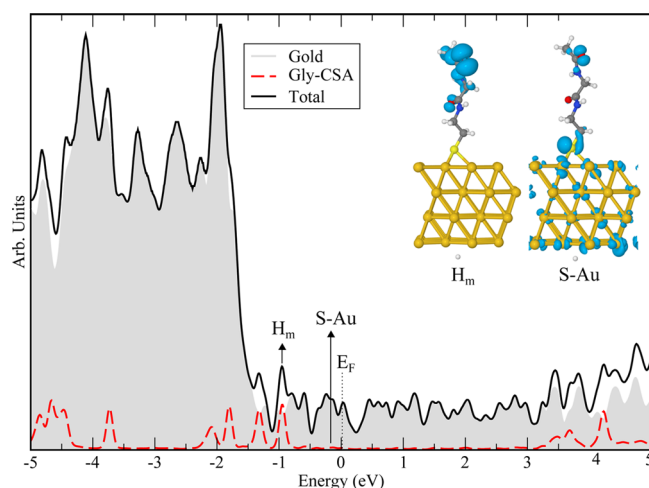


**Figure 3.** Total DOS (black line) and projected contributions on Au substrate (shaded area) and Gly-CSA molecule (red line) for the molecule/surface interface. Zero energy reference is set to Fermi energy ( $E_F$ ) of the system. Insets display two representative KS orbitals of the interface.

metal states, in agreement with the New-Andersen model,<sup>48</sup> routinely invoked for this kind of systems.

For the simulation of the Fc-Gly-CSA/Au(111) interface (Figure 1c), we started from the relaxed Gly-CSA/Au(111) configuration described above, including the Fc on the top of Gly-CSA. The whole structure was then fully relaxed. The presence of the Fc unit hardly modifies the atomic positions of the interface, leaving the S-Au bonds and the peptide bridge almost unchanged, as also can be seen from the almost untouched atomic charge of the sulfur atom (Table S1). On the contrary, the inclusion of ferrocene has a remarkable effect on the electronic structure of the interface (Figure 4). As in the previous case, we can distinguish a molecular peak stemming from the  $H_m$  orbital of the peptide fragment, just slightly shifted, of ~0.5 eV, toward lower energies. Analogously, low-intensity contributions similar to the S-Au states of Figure 3 can be observed at the Fermi energy. Yet, the top of the valence

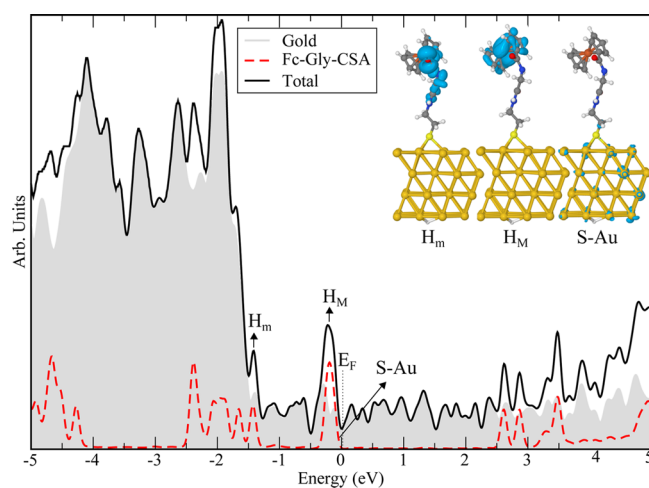


**Figure 4.** Total DOS (black line) and projected contributions on the Au substrate (shaded area) and Fc-Gly-CSA molecule (red line) for the molecule/surface interface. Zero energy reference is set to Fermi energy ( $E_F$ ) of the system. Insets display three representative KS orbitals of the interface.



band is now dominated by the same manifold of states ( $H_M$ ) localized on the Fc group, discussed in Figure 2b.

Even though the present simulations do not explicitly describe the electron transfer process, our results indicate a net and preferential route for charge transfer, in agreement with the experimental findings. We can summarize the ET mechanism as follows: the adsorption of the molecule involves a partial hybridization of the thiol states with the  $sp$  band of the Au(111) surface, as well as lower energy states a few eV below the Fermi energy. Most important, the formation of the interface does not affect the  $H_M$  manifold that maintains its molecular-like character. The small differences between the calculated ionization potential of the Fc moiety ( $\sim 6.0$  eV) and the work function of gold ( $\sim 5.1$  eV) pin the  $H_M$  close ( $\sim 0.2$  eV) to the Fermi energy of the system. This is a suitable electronic prerequisite to support an ET process. In fact, as a small external field is applied, the molecule, being energetically so close to the Fermi energy, oxidizes through electron transfer from the Fc to gold, as observed in the experiments. The localization of  $H_M$  states on the Fc and the absence of an electronic orbital contribution along the peptide chain sustain the hypothesis of a direct tunneling: there are no intermediate states localized on the Gly-CSA bridge close to the Fermi energy that could give support to the hopping mechanism. This does not imply that the peptide chain does not affect the characteristics of the systems. For instance, the presence of an intrinsic dipole moment of Gly-CSA affects the intermolecular coupling and drives the geometry and the density of the SAM. Furthermore, a directional dipole, acting as a rectifying potential, may foster the ET between Fc and gold and block the back transfer. Finally, the length of the bridge chain affects the tunneling barrier the electron must pass through in the ET process.<sup>21</sup>

In order to check the robustness of our results we considered, in addition, the effect of solvent and salt on the band alignment of the interface. To this aim we first included an explicit methanol solvent in the simulation cell. The results are displayed in Figure 5a, where we can easily recognize all the molecular features described above. In fact, we detect the hybridized S–Au orbitals that characterize the energy region across the Fermi energy, as well as the Gly-CSA HOMO-derived orbital  $H_m$  at  $-1.4$  eV. Furthermore, the presence of the solvent does not change the character and the energy position of the Fc-derived manifold  $H_M$  close to the Fermi energy. The inclusion of methanol molecules introduces spectral features over a large energy range in the DOS, including the Fermi region. As shown in the inset of Figure 5, these contributions do not directly participate in the ET processes. We further note that in the experimental samples the formation of SAM layers keeps the solvent molecules far away from the surface, preventing (or reducing) the direct contact with the substrate.<sup>3,24</sup>

The scenario is maintained also when sodium-perchlorate salt is diluted in the solution (Figure 5b). In the absence of an external electric field,  $Na^+$  and  $ClO_4^-$  do not directly interact with the Fc-Gly-CSA and do not perturb the  $H_M$  peak, responsible for the Fc-to-Au charge transfer. Their presence introduces occupied molecular states at  $-1.7$  eV below the Fermi energy and imparts an electrostatic shift of the methanol states that are no longer superimposed, in energy, to the Fc peak  $H_M$ , confirming that neither the solvent nor the salt directly participates in the ET transfer mechanism. Again, this can be quantified by the charges on the involved atoms that

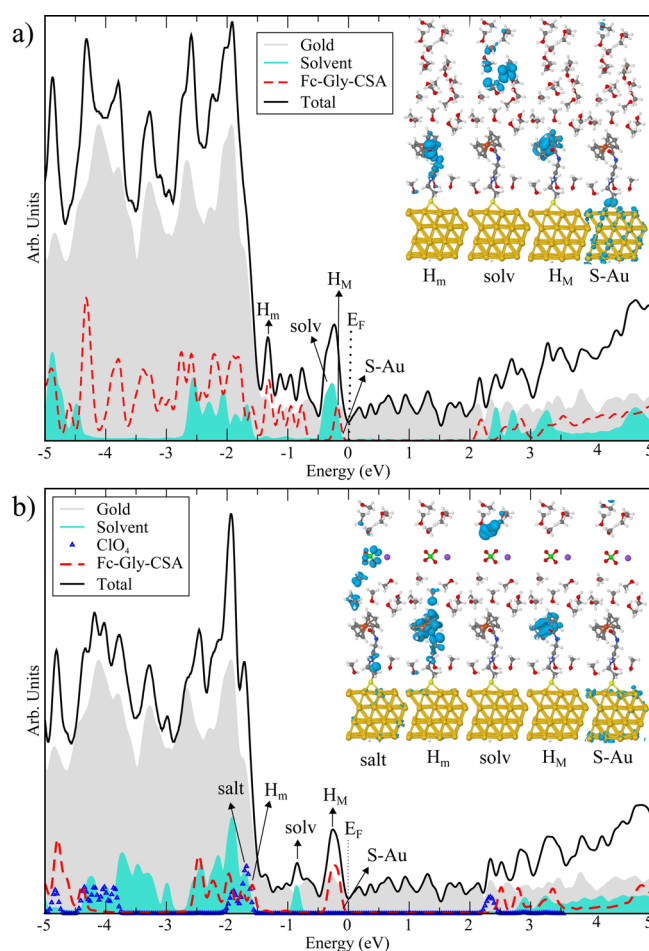


**Figure 5.** Total DOS (black line) and projected contributions on the Au substrate (shaded area) and Fc-Gly-CSA molecule (red line) for the molecule/surface interface: (a) including methanol solvent (cyan area); (b) including sodium perchlorate (blue line) and methanol solvent. Zero energy reference is set to the Fermi energy ( $E_F$ ) of the system. Insets display representative KS orbitals of the interface.

show no charge transfer at all (Table S1, Supporting Information). Instead, the role of  $Na^+$  and  $ClO_4^-$  becomes crucial during the ET process, in order to compensate the final positive charge of the oxidized Fc group and the negative charge of the reduced counter-electrode of the experimental electrochemical cell.

As shown in Table S2 (Supporting Information), the LOMO–HOMO energy difference for the Fc-Gly-CSA molecule is very stable and does not change upon interaction with the Au(111) neither with the solvent and/or salt.

## CONCLUSIONS

We have presented the theoretical investigation of the Fc-Gly-CSA attached to the Au(111) surface. To our knowledge, this is the first simulation that analyzes the ET mechanism of Fc-SAMs in a gold surface from first principles. We gradually introduced more components and systematically analyzed the possible changes in the electronic structure, providing a comprehensive and systematic study which considers most of the important effects to the charge transfer mechanism. The obtained results have shown consistency in all cases. When comparing Gly-CSA/Au(111) and Fc-Gly-CSA/Au(111) it was noted that the electronic states of the molecule that appears

close to, but always below, the Fermi energy are localized on the Fc units and do not extend to the peptide chain. It is furthermore seen that the salt inclusion is determinant to correctly describe solvent effects. In all cases we do not find evidence for the role of the peptide chain on the electron transfer process; however, the thiol group is seen to take part on the level alignment through metal–molecule bonding. In addition, the energy difference between the states  $H_m$  and  $H_M$  is sufficiently large to strongly support the robustness of our results against fluctuations of the system. The band alignment, which places the Fc moiety HOMO level below the Au Fermi energy, indicates that an applied electric field, as in a cyclic voltammetry experiment, should be able to promote band bending close to the  $E_F$ , transferring electrons from the Fc to the Au(111). Even if we did not address finite temperature effects, the investigations performed here provide strong evidence for electron tunneling in the assembled Fc-Gly-CSA/Au(111) surface in a solvent environment.

## ■ ASSOCIATED CONTENT

### ■ Supporting Information

Additional results for the Löwdin charges and LOMO–HOMO differences. This material is available free of charge via the Internet at <http://pubs.acs.org>.

## ■ AUTHOR INFORMATION

### Corresponding Author

\*E-mail: [hmpetrl@if.usp.br](mailto:hmpetrl@if.usp.br).

### Notes

The authors declare no competing financial interest.

## ■ ACKNOWLEDGMENTS

The authors acknowledge computing time provided on the Blue Gene/P supercomputer supported by the Research Computing Support Group (Rice University) and Laboratório de Computação Científica Avançada (Universidade de São Paulo). This work was financially supported by FAPESP (project: 2012/02326-8), CNPq, INCT-INEO, and Rede Nanobiomed (CAPES).

## ■ REFERENCES

- (1) Eckermann, A. L.; Feld, D. J.; Shaw, J. A.; Meade, T. J. Electrochemistry of Redox-Active Self-Assembled Monolayers. *Coord. Chem. Rev.* **2010**, *254*, 1769–1802.
- (2) Kitagawa, K.; Morita, T.; Kimura, S. Electron Transfer in Metal-Molecule-Metal Junction Composed of Self-Assembled Monolayers of Helical Peptides Carrying Redox-Active Ferrocene Units. *Langmuir* **2005**, *21*, 10624–10631.
- (3) Orlowski, G. A.; Chowdhury, S.; Kraatz, H.-B. Reorganization Energies of Ferrocene-Peptide Monolayers. *Langmuir* **2007**, *23*, 12765–12770.
- (4) Takeda, K.; Morita, T.; Kimura, S. Effects of Monolayer Structures on Long-Range Electron Transfer in Helical Peptide Monolayer. *J. Phys. Chem. B* **2008**, *112*, 12840–12850.
- (5) Ariga, K.; Hill, J. P.; Lee, M. V.; Vinu, A.; Charvet, R.; Acharya, S. Challenges and Breakthroughs in Recent Research on Self-Assembly. *Sci. Technol. Adv. Mater.* **2008**, *9*, 014109(96pp).
- (6) Yokota, Y.; Yamada, T.; Kawai, M. Ion-Pair Formation Between Ferrocene-Terminated Self-Assembled Monolayers and Counteranions Studied by Force Measurements. *J. Phys. Chem. C* **2011**, *115*, 6775–6781.
- (7) Martins, M. V. A.; Pereira, A. R.; Luz, R. A. S.; Iost, R. M.; Crespihlo, F. N. Evidence of Short-Range Electron Transfer of a

Redox Enzyme on Graphene Oxide Electrodes. *Phys. Chem. Chem. Phys.* **2014**, *1*–11.

- (8) Saweczko, P.; Enright, G. D.; Kraatz, H. B. Interaction of Ferrocenyl-Dipeptides with 3-Aminopyrazole Derivatives: Beta-Sheet Models? A Synthetic, Spectroscopic, Structural, and Electrochemical Study. *Inorg. Chem.* **2001**, *40*, 4409–4419.

- (9) Galka, M. M.; Kraatz, H.-B. Electron Transfer Studies on Self-Assembled Monolayers of Helical Ferrocenyl-Oligoproline-Cysteine Bound to Gold. *ChemPhysChem* **2002**, *3*, 356–359.

- (10) Morita, T.; Kimura, S. Long-Range Electron Transfer over 4 Nm Governed by an Inelastic Hopping Mechanism in Self-Assembled Monolayers of Helical Peptides. *J. Am. Chem. Soc.* **2003**, *125*, 8732–8733.

- (11) Smalley, J. F.; Finklea, H. O.; Chidsey, C. E. D.; Linford, M. R.; Creager, S. E.; Ferraris, J. P.; Chalfant, K.; Zawodzinski, T.; Feldberg, S. W.; Newton, M. D. Heterogeneous Electron-Transfer Kinetics for Ruthenium and Ferrocene Redox Moieties Through Alkanethiol Monolayers on Gold. *J. Am. Chem. Soc.* **2003**, *125*, 2004–2013.

- (12) Orlowski, G. A.; Chowdhury, S.; Long, Y.-T.; Sutherland, T. C.; Kraatz, H.-B. Electrodeposition of Ferrocenyl Peptide Disulfides. *Chem. Commun.* **2005**, *2*, 1330–1332.

- (13) Mandal, H. S.; Kraatz, H.-B. Electron Transfer Across  $\alpha$ -Helical Peptides: Potential Influence of Molecular Dynamics. *Chem. Phys.* **2006**, *326*, 246–251.

- (14) Wilks, R. G.; MacNaughton, J. B.; Kraatz, H.-B.; Regier, T.; Moewes, A. Combined X-Ray Absorption Spectroscopy and Density Functional Theory Examination of Ferrocene-Labeled Peptides. *J. Phys. Chem. B* **2006**, *110*, 5955–5965.

- (15) Orlowski, G. A.; Chowdhury, S.; Kraatz, H.-B. the Effect of Alkali Metal Ions on the Electrochemical Behavior of Ferrocene-Peptide Conjugates Immobilized on Gold Surfaces. *Electrochim. Acta* **2007**, *53*, 2034–2039.

- (16) Kai, M.; Takeda, K.; Morita, T.; Kimura, S. Distance Dependence of Long-Range Electron Transfer Through Helical Peptides. *J. Pept. Sci.* **2008**, *14*, 192–202.

- (17) Okamoto, S.; Morita, T.; Kimura, S. Electron Transfer Through A Self-Assembled Monolayer of A Double-Helix Peptide with Linking the Terminals by Ferrocene. *Langmuir* **2009**, *25*, 3297–3304.

- (18) Brooksby, P. A.; Anderson, K. H.; Downard, A. J.; Abell, A. D. Electrochemistry of Ferrocenyl Beta-Peptide Monolayers on Gold. *Langmuir* **2010**, *26*, 1334–1339.

- (19) Norman, L. L.; Badia, A. Microcantilevers Modified with Ferrocene-Terminated Self-Assembled Monolayers: Effect of Molecular Structure and Electrolyte Anion on the Redox-Induced Surface Stress. *J. Phys. Chem. C* **2011**, *115*, 1985–1995.

- (20) Martí, S.; Labib, M.; Shipman, P. O.; Kraatz, H.-B. Ferrocene-Peptide Conjugates: From Synthesis to Sensory Applications. *Dalton Trans.* **2011**, *40*, 7264–7290.

- (21) Mandal, H. S.; Kraatz, H.-B. Electron Transfer Mechanism in Helical Peptides. *J. Phys. Chem. Lett.* **2012**, *3*, 709–713.

- (22) Pawlowski, J.; Juhaniewicz, J.; Tymecka, D.; Sek, S. Electron Transfer Across  $\alpha$ -Helical Peptide Monolayers: Importance of Interchain Coupling. *Langmuir* **2012**, *28*, 17287–17294.

- (23) Maeda, H.; Sakamoto, R.; Nishihara, H. Metal Complex Oligomer and Polymer Wires on Electrodes: Tactical Constructions and Versatile Functionalities. *Polymer* **2013**, *54*, 4383–4403.

- (24) Kraatz, H.-B. Ferrocene-Conjugates of Amino Acids, Peptides and Nucleic Acids. *J. Inorg. Org. Polym. Mater.* **2005**, *15*, 83–106.

- (25) Bediako-Amoa, I.; Silerova, R.; Kraatz, H.-B. Ferrocenyl Glycylcystamine: Organization into a Supramolecular Helicate Structure Extensive Intermolecular Hydrogen Bonding in Ferrocenyl Glycylcystamine Gives Rise to a Novel Ordered Double Helical Arrangement with a Helical Pitch Height of 14 Å. *Chem. Commun.* **2002**, 2430–2431.

- (26) Marcus, R. A. On the Theory of Electron-Transfer Reactions. VI. Unified Treatment for Homogeneous and Electrode Reactions. *J. Chem. Phys.* **1965**, *43*, 679–701.

- (27) Marcus, R.; Sutin, N. Electron Transfers in Chemistry and Biology. *Biochim. Biophys. Acta* **1985**, *811*, 265–322.

- (28) Polo, F.; Antonello, S.; Formaggio, F.; Toniolo, C.; Maran, F. Evidence Against the Hopping Mechanism as an Important Electron Transfer Pathway for Conformationally Constrained Oligopeptides. *J. Am. Chem. Soc.* **2005**, *127*, 492–493.
- (29) Watanabe, J.; Morita, T.; Kimura, S. Effects of Dipole Moment, Linkers, and Chromophores at Side Chains on Long-Range Electron Transfer Through Helical Peptides. *J. Phys. Chem. B* **2005**, *109*, 14416–14425.
- (30) Malak, R. A.; Gao, Z.; Wishart, J. F.; Isied, S. S. Long-Range Electron Transfer Across Peptide Bridges: the Transition From Electron Superexchange to Hopping. *J. Am. Chem. Soc.* **2004**, *126*, 13888–13889.
- (31) Filippini, G.; Goujon, F.; Bonal, C.; Malfreyt, P. Toward A Prediction of the Redox Properties of Electroactive SAMs: A Free Energy Calculation by Molecular Simulation. *J. Phys. Chem. B* **2010**, *114*, 12897–12907.
- (32) Doneux, T.; Bouffier, L.; Mello, L. V.; Rigden, D. J.; Kejnovská, I.; Fernig, D. G.; Higgins, S. J.; Nichols, R. J. Molecular Dynamics and Electrochemical Investigations of a PH-Responsive Peptide Monolayer. *J. Phys. Chem. C* **2009**, *113*, 6792–6799.
- (33) Ahn, Y.; Saha, J. K.; Schatz, G. C.; Jang, J. Molecular Dynamics Study of the Formation of a Self-Assembled Monolayer on Gold. *J. Phys. Chem. C* **2011**, *115*, 10668–10674.
- (34) Goujon, F.; Bonal, C.; Limoges, B.; Malfreyt, P. Molecular Dynamics Simulations of Ferrocene-Terminated Self-Assembled Monolayers. *J. Phys. Chem. B* **2010**, *114*, 6447–6454.
- (35) Heck, A.; Woiczikowski, P. B.; Kubař, T.; Giese, B.; Elstner, M.; Steinbrecher, T. B. Charge Transfer in Model Peptides: Obtaining Marcus Parameters from Molecular Simulation. *J. Phys. Chem. B* **2012**, *116*, 2284–2293.
- (36) Roy, L. E.; Jakubikova, E.; Guthrie, M. G.; Batista, E. R. Calculation of One-Electron Redox Potentials Revisited. Is it Possible to Calculate Accurate Potentials with Density Functional Methods? *J. Phys. Chem. A* **2009**, *113*, 6745–6750.
- (37) Yu, J.; Huang, D. M.; Shapter, J. G.; Abell, A. D. Electrochemical and Computational Studies on Intramolecular Dissociative Electron Transfer in  $\beta$ -Peptides. *J. Phys. Chem. C* **2012**, *116*, 26608–26617.
- (38) Kohn, W.; Sham, L. J. Self-Consistent Equations Including Exchange and Correlation Effects. *Phys. Rev.* **1965**, *140*, A1133–A1138.
- (39) Iori, F.; Di Felice, R.; Molinari, E.; Corni, S. GolP: An Atomistic Force-Field to Describe the Interaction of Proteins with Au(111) Surfaces in Water. *J. Comput. Chem.* **2009**, *30*, 1465–1476.
- (40) Cicero, G.; Calzolari, A.; Corni, S.; Catellani, A. Anomalous Wetting Layer at the Au(111) Surface. *J. Phys. Chem. Lett.* **2011**, *2*, 2582–2586.
- (41) Calzolari, A.; Felice, R. D. Surface Functionalization Through Adsorption of Organic Molecules. *J. Phys. Condens. Matter* **2007**, *19*, 305018 (11pp).
- (42) Giannozzi, P.; et al. QUANTUM ESPRESSO: A Modular and Open-Source Software Project for Quantum Simulations of Materials. *J. Phys. Condens. Matter* **2009**, *21*, 395502 (19pp).
- (43) Perdew, J. P.; Burke, K.; Ernzerhof, M. Generalized Gradient Approximation Made Simple. *Phys. Rev. Lett.* **1996**, *77*, 3865–3868.
- (44) Vanderbilt, D. Soft Self-Consistent Pseudopotentials in a Generalized Eigenvalue Formalism. *Phys. Rev. B* **1990**, *41*, 7892–7895.
- (45) Baldereschi, A.; Baroni, S.; Resta, R. Band Offsets in Lattice-Matched Heterojunctions: A Model and First-Principles Calculations for GaAs/AlAs. *Phys. Rev. Lett.* **1988**, *61*, 734–737.
- (46) Peressi, M.; Binggeli, N.; Baldereschi, A. Band Engineering at Interfaces: Theory and Numerical Experiments. *J. Phys. D: Appl. Phys.* **1998**, *31*, 1273–1299.
- (47) Pedretti, A.; Villa, L.; Vistoli, G. VEGA ZZ - an Open Platform to Develop Chemo-Bio-Informatics Applications, Using Plug-in Architecture and Script Programming. *J. Comput.-Aided Mol. Des.* **2004**, *18*, 167–173.
- (48) Di Felice, R.; Selloni, A. Adsorption Modes of Cysteine on Au(111): Thiolate, Amino-Thiolate, Disulfide. *J. Chem. Phys.* **2004**, *120*, 4906–4914.